Studies towards the development of a PET radiotracer for imaging of the P2Y1 receptors in the brain: synthesis, 18F-labeling and preliminary biological evaluation

Moldovan, R.-P.; Wenzel, B.; Teodoro, R.; Neumann, W.; Dukic-Stefanovic, S.; Deuther-Conrad, W.; Hey-Hawkins, E.; Krügel, U.; Brust, P.;

Originally published:

March 2019

European Journal of Medicinal Chemistry (2019), 142-159

DOI: https://doi.org/10.1016/j.ejmech.2019.01.006

Development of a PET radiotracer for imaging of the purinergic $P2Y_1$ receptors in the brain: synthesis, ^{18}F-labelling and preliminary biological evaluation

Rareş-Petru Moldovan[a,*], Barbara Wenzel[a], Rodrigo Teodoro[a], Wilma Neumann[c], Sladjana Dukic-Stefanovic[a], Winnie Deuther-Conrad[a], Evamarie Hey-Hawkins[b], Ute Krügel[c§] and Peter Brust[a§]

[a] *Institute of Radiopharmaceutical Cancer Research, Helmholtz-Zentrum Dresden-Rossendorf e. V., Permoserstrasse 15, Leipzig 04318, Germany*
[b] *Institut für Anorganische Chemie, Fakultät für Chemie und Mineralogie, Universität Leipzig, Leipzig 04103, Germany*
[c] *Rudolf Boehm Institute of Pharmacology and Toxicology, Medical Faculty, Universität Leipzig, Leipzig 04107, Germany*
[§] Equal contribution
Corresponding author. Helmholtz-Zentrum Dresden-Rossendorf e. V., Institute of Radiopharmaceutical Cancer Research, Permoserstrasse 15, Leipzig 04318, Germany. Phone: +49-341-234-179-4634; E-mail address: r.moldovan@hzdr.de (R.-P. Moldovan).

ABSTRACT: Purine nucleotides such as ATP and ADP are important extracellular signaling molecules in almost all tissues. Via $P2Y_1R$ activation they mediate brain functions by trophic effects like differentiation and proliferation but also via fast synaptic transmission. The understanding of its role in brain disorders is limited because of lack of suitable brain-penetrating $P2Y_1R$-selective drugs. In this paper we describe the first efforts to develop an ^{18}F-PET tracer and a boron based neutron capture therapeutic (NCT) agent starting from the structure of the highly affine and selective, non-nucleotidic $P2Y_1R$ ligand 1-(2-(2-(*tert*-butyl)phenoxy)pyridin-3-yl)-3-(4-(trifluoromethoxy)phenyl)urea (**8**). A small series of fluorinated compounds was developed by modifying the *p*-(trifluoromethoxy)phenyl subunit of the lead compound **8**. Additionally, the *p*-(trifluoromethoxy)phenyl subunit was substituted by carbaboran, a boron rich cluster with potential applicability in neutron capture therapy (NCT). The *in vitro* pharmacological study revealed the fluorinated derivative **16** with 8.2-fold higher antagonistic potency than the lead compound **8**. Compound [^{18}F]**16** was radiosynthesized by using tetrabutylammonium [^{18}F]fluoride ([^{18}F]TBAF) starting from the corresponding ethyltosylate **15** and was obtained with a radiochemical purity of ≥ 99%, in radiochemical yields (EOB) of 28.2 ± 0.8% (n = 4, decay corrected), molar activities (EOS) in the range of 153-283 GBq/µmol using starting activities of 2-3 GBq. First *in vivo* investigation revealed fast metabolization of [^{18}F]**16** and nearly no intact radiotracer could be detected in plasma and brain samples of a CD-1 mouse at 30 minutes post injection. Nevertheless, the high binding affinity and selectivity makes this class of compounds interesting for further optimizations toward the development of a $P2Y_1$-PET radiotracer for brain imaging.

Keywords: Purinergic receptors, $P2Y_1$, radiotracer, positron emission tomography, radiometabolites

Graphical abstract

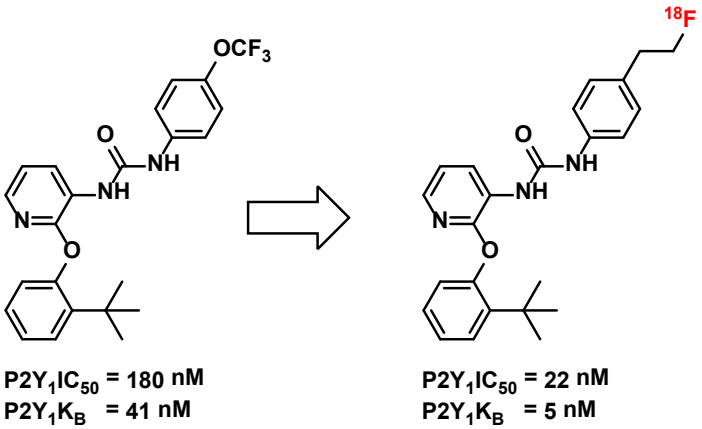

1. Introduction

Purinergic receptors are a family of plasma membrane proteins that are found in almost all mammalian tissue including brain.[1-3] They are subdivided in the P1 (adenosine receptors), with adenosine as endogenous ligand and P2 receptors which are subdivided in P2X[4] and P2Y[5] receptor families. P2X receptors are ligand-gated ion channels, activated endogenously preferentially by ATP[6-8] while P2Y are G-protein coupled receptors (GPCR)[9] with ATP and ADP as main endogenous ligands.[10] Cellular stimulation triggers ATP release which either interacts with specific purinergic receptors or it is degraded to ADP, AMP and then to adenosine, which interact with the different purinergic receptors at the cell surface therefore regulating or modulating cellular functions.[11] Metabotropic P2Y receptors, belonging to the rhodopsin-like GPCR family which are mediating the fast cell-to-cell signaling and also trophic effects.[12] To date, eight P2Y receptor subtypes have been characterized and cloned in human, namely $P2Y_1$, $P2Y_2$, $P2Y_4$, $P2Y_6$, $P2Y_{11}$, $P2Y_{12}$, $P2Y_{13}$ and $P2Y_{14}$.[5, 10, 13] In particular, the $P2Y_1R$[14] subtype is involved in various physiological and pathophysiological processes in the brain.[15] They are characterized by a broad and high density distribution in several brain regions and are involvement in diseases such as epilepsy,[16] traumatic brain injury, ischemia, AD, and also cancer.[17-19] However, the exact understanding of the role of the $P2Y_1R$ as useful pharmacological tools to investigate brain is limited.[15, 20] To further investigate the involvement of $P2Y_1R$ in pathologic brain conditions and to study the chemical and biological properties of the $P2Y_1R$ a radioligand with PET applicability is needed.

Given the nucleotidic nature of the ADP (**1**, Figure 1), the endogenous $P2Y_1R$ ligand, numerous synthetic ligands with similar structural skeleton and even subnanomolar affinity and high selectivity for the $P2Y_1R$ were developed to date.[13, 21, 22] Although ADP itself is a rather weak and non-selective agonist at the $P2Y_1R$, chemical modifications of this molecule led to candidates applicable to prove $P2Y_1R$ as potential therapeutic target (compounds **2**, **3** and **4**, Figure 1A).[22, 23] Since nucleotidic ligands are thought not to pass the blood brain barrier in a sufficient amount because of their negative charge at neutral pH, they cannot be considered for development of PET tracers for brain imaging.[24-26] On the other hand, only a few non-nucleotidic $P2Y_1R$ ligands with sub-micromolar affinity have been reported to

date.[27-29] As a predominant scaffold diarylurea plays a crucial rolefor the binding to the $P2Y_1R$ (Figure 1). For instance compound **5** (K_i = 10 nM) was reported by Pfizer laboratories as a result of a SAR study performed for the optimization of a lead molecule identified by a high throughput screening (HTS).[29] Similarly, GlaxoSmithKline laboratories identified compound **6**[27] with micromolar affinity (K_i = 600 nM) and Bristol-Myers Squibb (BMS) laboratories which disclosed compound **7** (K_i = 75 nM, Figure 1).[13, 30]

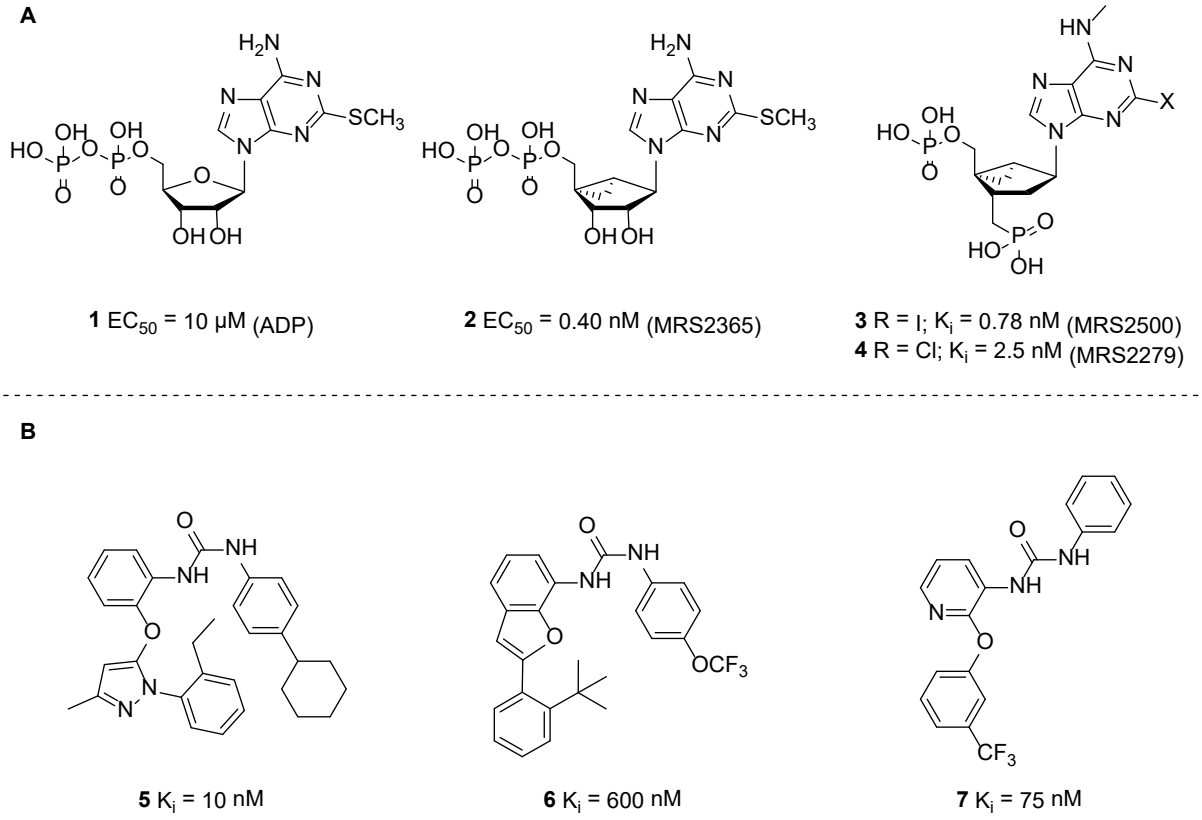

Figure 1. The endogenous ligand ADP (**1**) and selected $P2Y_1R$ (**A**) nucleotidic and (**B**) non-nucleotidic ligands.

Compound **7** was identified by screening of >1 million compounds and an initial SAR study on this molecule lead to the development of compound **8** (Figure 2) with high affinity (K_i = 6 nM) and selectivity for the $P2Y_1R$.[30] It shows good metabolic stability when incubated with human and rat liver microsomes. This class of non-nucleotidic $P2Y_1R$ ligands has been extended by substantial SAR studies accounting more than 150 members reported to date.[30-35] During this study performed by BMS laboratories, all parts of the molecule were modified and investigated for physiochemical and biological impact aiming at the development of a candidate for clinical trials.[30-35] Furthermore, the binding mode of **8** to the $P2Y_1R$ was elucidated by X-ray crystallography and the molecular mechanism of receptor activation has been studied,[36, 37] providing valuable information for computational driven pharmacological developments.[38] Recently, the impact of the allosteric binding mode of **8** on the $P2Y_1R$ signaling patterns was investigated.[39]

The occasionally low nanomolar $P2Y_1R$ affinity and the non-nucleotidic nature these diaryl urea ligands are qualifying this scaffold as the best starting point for the development of an ^{18}F-labeled radiotracer for PET imaging of the cerebral $P2Y_1R$. A main challenge in the

development of a radiofluorinated ligand is the introduction of a fluorine atom with retention of the binding affinity, at a position which allows a facile, late stage incorporation of the ^{18}F atom.[26] Ideally also the formation of brain penetrant radiometabolites should be prevented. Considering the structure of the lead molecule **8** and SAR study previously performed on this template, the modification of the phenyl ring directly attached at the urea subunit appears to have only a low impact on the binding affinity of these compounds. Analogously to compounds **9** and **10** (Figure 2),[30] the introduction of a fluoroethyl or a fluoroethoxy group should be tolerated at the phenyl 4-position, enabling a facile S_N2 radiofluorination at aliphatic position. Aiming at a deep through investigation of this scaffold, the replacement of the urea subunit by a metabolically more stable heterocycle like thiazole has also been taken into acount.[31]

Beside the potential as diagnostic tool for PET, it is worthwhile to explore the therapeutic potential of this scaffold by taking advantage of a unique technique like neutron capture therapy (NCT). For this, a boron rich moiety should be implemented at a position of the molecule, ideally, without causing alteration of the binding affinity towards the $P2Y_1$ receptors. Recently, we reported the possibility to replace the phenyl ring with a carbaborane moiety for established cyclooxygenase (COX) inhibitors.[40-42] As possible strategy to develop such a compound would be to replace compound's **8** *p*-(trifluoromethoxy)phenyl subunit by a carbaborane, a boron rich scaffold with potential applicability in NCT. (not shown in Figure 2, see Scheme 3).

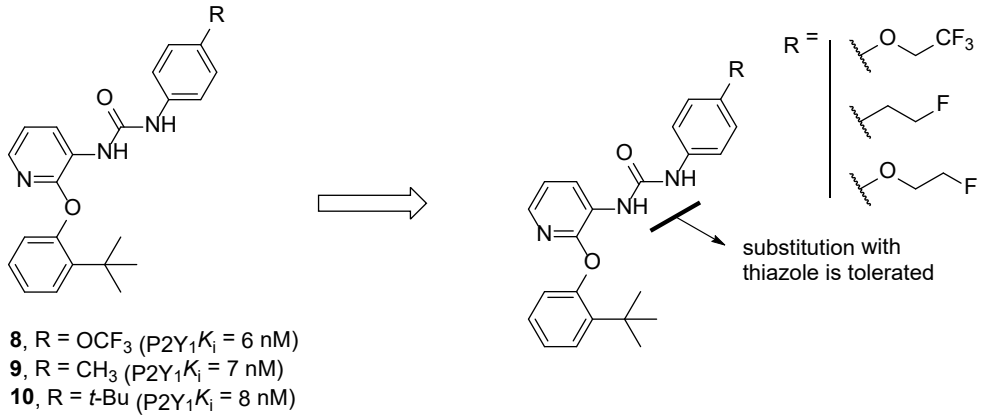

Figure 2. The structure of compounds **8**, **9** and **10** and proposed fluoro-derivatization.[30, 31]

2. Results and discussion

2.1 Chemistry

The synthesis of the lead compound **8** (Figure 2 and Scheme 1) was performed as described by BMS with small modifications.[30] The coupling of the 2-*tert* butylphenol (**10**) with pyridine **11** in presence of Cs_2CO_3 was followed by Pd/C-H_2 nitro group reduction to the corresponding amine **12** and subsequently treatment with diphosgene in presence of Et_3N to give the isocyanate key intermediate **13** in 55% yield over three steps. The herein obtained isocyanate was coupled without further purification with different amines to give urea derivatives **8**, **14** and **17** in high yields (>70%, see Experimental section). The fluoroethyl compound **16** was obtained from **14** by tosylation and subsequent fluorination with TBAF. The mono and tri-fluoroethoxylated derivatives **18** and **19** were obtained from phenol **17**

(Scheme 1). With large amounts of compound **12** in our hands, we also built the 2-aminothiazole ring as previously described[31] aiming to reinforce the poor metabolic stability of the urea group. For this, compound **12** was treated with benzoyl isothiocyanate, hydrolyzed in presence of LiOH and cyclized with 3-bromo-1,1,1-trifluoropropan-2-one in presence of base at elevated temperature to give **20**. Bromination at the thiazole 5-position of **20** gave the suitable precursor for the Suzuki Coupling. At this point, we decided to introduce the fluorine atom at the second position of a pyridine ring due to the facile radiofluorination at this position. We randomly had chosen the 2-fluoropyridin-5-boronic acid as coupling partner for the Suzuki reaction[43, 44] and thus, compound **21** was obtained in 78 % yield (Scheme 1).

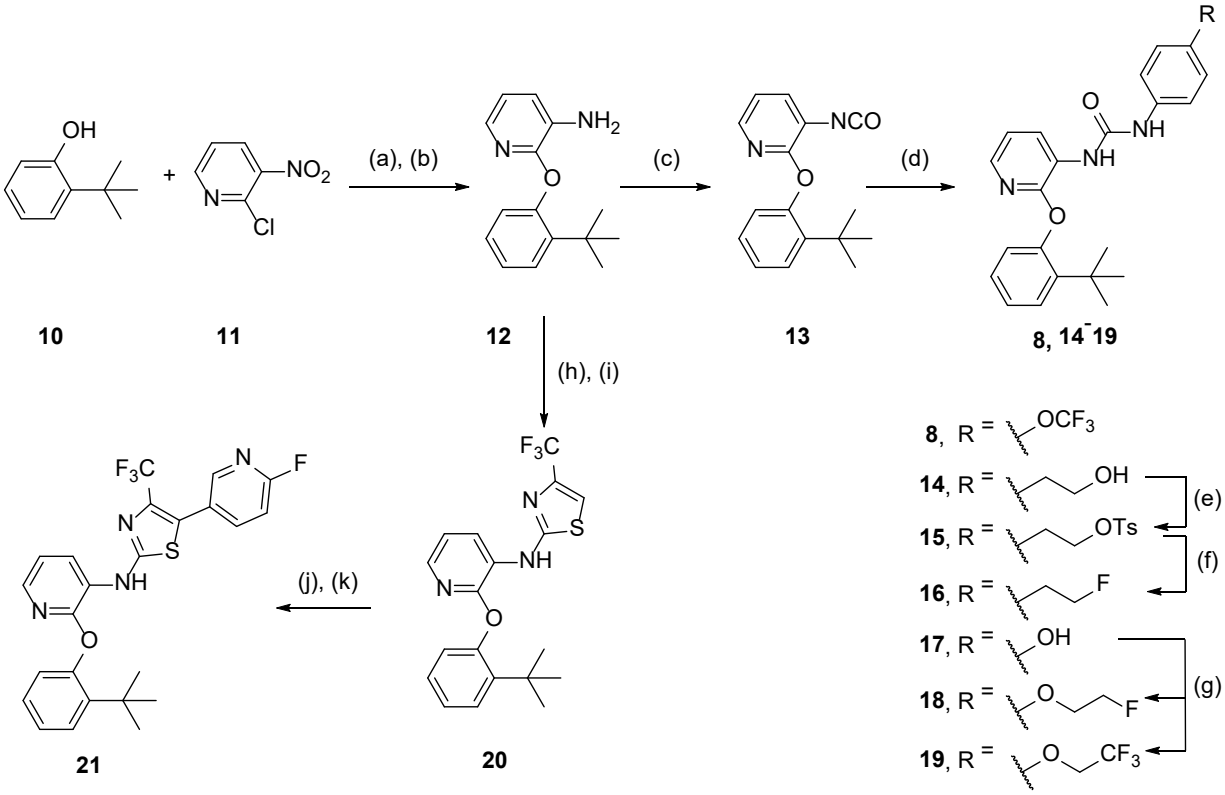

Scheme 1. Synthesis of the diaryl urea derivatives **8**, **14-19** and 2-aminothiazole **21**. (a) Cs_2CO_3, DMF, 70 °C, 14 h; (b) Pd/C, H_2; (c) diphosgene, Et_3N, DCM, 0 °C to rt., 2 h; (d) corresponding substitute aniline, toluol, 80 °C, 1 h; (e) TsCl, pyridine, DCM, rt, 16 h; (f) TBAF, THF, rt, 16 h; (g) RX, K_2CO_3, CH_3CN, 80 °C, 16 h; (h) i. benzoyl isothiocyanate, DCM, 40 °C, 2 h; ii. 2M LiOH/MeOH, 50 °C, 2 h; (i) 3-bromo-1,1,1-trifluoropropan-2-one, 2,6-lutidine, EtOH, 80 °C, 24 h; (j) NBS, AcOH/THF, 0 °C, 2 h; (k) Suzuki Coupling using $Pd(PPh_3)_4$, Na_2CO_3, toluene/EtOH, 95 °C, 16 h.

Additionally, the *p*-(trifluoromethoxy)phenyl of compound **8** subunit was replaced with carbaborane by using amino-carbaborane **22** as coupling partner of the isocyanate **13**. Carbaborane **22** was obtained by a literature known protocol from the commercially available *o*-carborane.[45] It is worthwhile to mention that in this case the urea group formation was much slower (24 h) as observed for the rest of the urea derivatives shown in this paper probably due

to the low nucleophilicity the amino-carbaborane **22**. In case of $P2Y_1R$ potency, compound **23** could be investigated for its potential as NCT therapeutic agent.

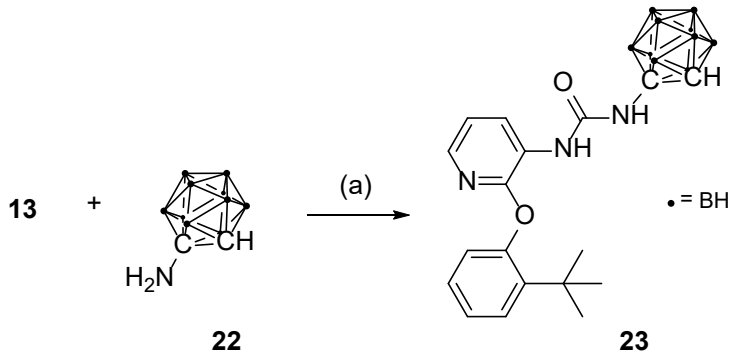

Scheme 3. Synthesis of the carbaborane derivative **23**. a) toluol, 80 °C, 24 h.

2.2 In vitro biological evaluation

The herein newly described derivatives **16**, **18**, **19** and **23** together with the literature known compound **8** were tested for *in vitro* pharmacology in a commercially available CEREP $P2Y_1R$ cellular functional assay for both agonist and antagonist effects. A first assay was performed at one concentration point of the tested compound (2.0×10^{-8}, n = 2), using the known MRS2365, 2MeSATP and MRS2500 as reference compounds for the agonist and antagonist effect, respectively (see Table 1).[22] As shown in Table 1,[30] at this concentration the lead compound **8** shown no antagonist effect. The fluoroethyl and trifluoroethoxy derivatives **16** and **19** shown a slight increase in antagonist effect. As expected,[30] these compounds are devoid of agonist effect. To verify the results from Table 1, compounds **8**, **16** and **23** were subject of a detailed antagonist activity study. As shown in Figure 3, the fluorinated derivative **16** possess ~8-fold higher antagonistic potency than the starting compound **8**. The boron rich compound **23** is inactive. Thus compound **16** has $P2Y_1IC_{50}$ of 22 nM and a $P2Y_1K_B$ of 5 nM, where K_B is the estimated antagonist dissociations constant and was calculated with the Chang-Prusoff equation.[46]

Table 1. Cellular functional assays of antagonist and agonist effect at 20 nM compound concentration.

Compound	Antagonist Effect	Agonist Effect
8	0	-12.0[a]; 0.2[b]
16	15	-14.2[a]; -3.7[b]
18	5	-14.9[a]
19	12	-13.7[a]
21	2	-11.2[a]
23	0.8	0.2[b]

[a]Functional assay performed with MRS2365 as reference compound
[b]Functional assay performed with 2MeSATP as reference compound

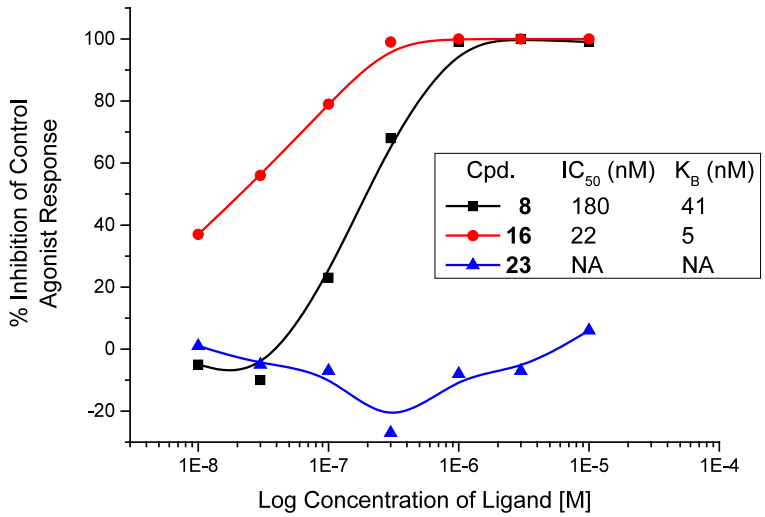

Figure 3. $P2Y_1$ antagonist effect of compounds **8** and **16** and **23**. (n = 2, NA = not applicable)

2.3 Radiochemistry

The new radioligand [^{18}F]**16** was prepared by nucleophilic substitution from the tosylate precursor (**15**, see Scheme 1) using anhydrous [^{18}F]tetra-*n*-butyl ammonium fluoride ([^{18}F]TBAF) in *tert*-BuOH (Scheme 4). Under conventional heating at 90 °C and 10 min reaction time no considerable increase of labelled product was observed, resulting in labelling efficiencies of 58.0 ± 6.4% (n = 5). Beside [^{18}F]fluoride, two radioactive by-products (< 15%

of total radioactivity) were observed according to radio-TLC analysis. Interestingly, when the classical K[^{18}F]F-$K_{2.2.2}$-carbonate complex system and acetonitrile (CH_3CN) at 90 °C were used, considerably lower labelling yields were achieved (< 9%). The precursor **15** remained stable under all conditions tested as proven by HPLC.

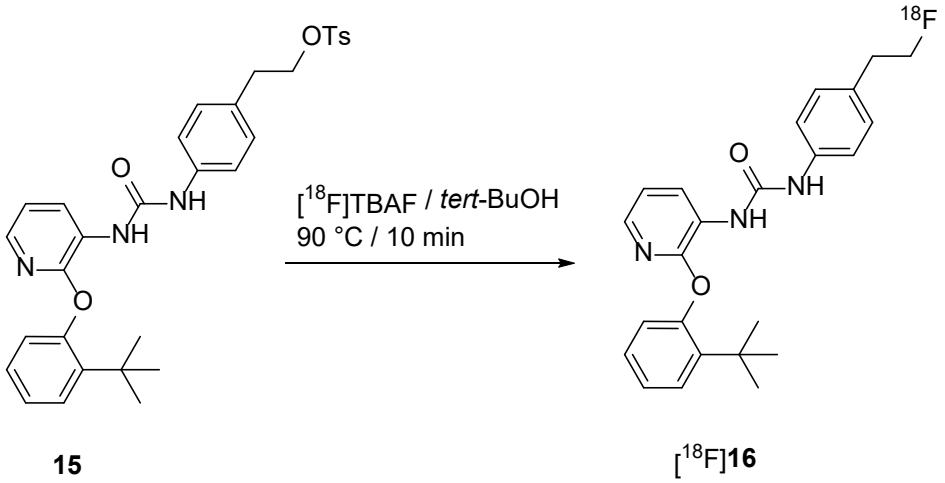

Scheme 4. ^{18}F-Radiolabelling of **15**.

The isolation of [^{18}F]**16** was performed by using semi-preparative RP-HPLC. The product was collected at a retention time of 25–29 min (see Figure 4A), purified using solid phase extraction on an RP cartridge and formulated in sterile isotonic saline containing 10% of EtOH for better solubility. Analytical radio- and UV-HPLC of the final product, spiked with the nonlabelled reference compound, confirmed the identity of [^{18}F]**16** (Figure 4B). Finally, the formulated radiotracer was obtained with a radiochemical purity of ≥ 99%, in radiochemical yields (EOB) of 28.2 ± 0.8% (n = 4, decay corrected), and molar activities (EOS) in the range of 153–283 GBq/µmol using starting activities of 2-3 GBq.

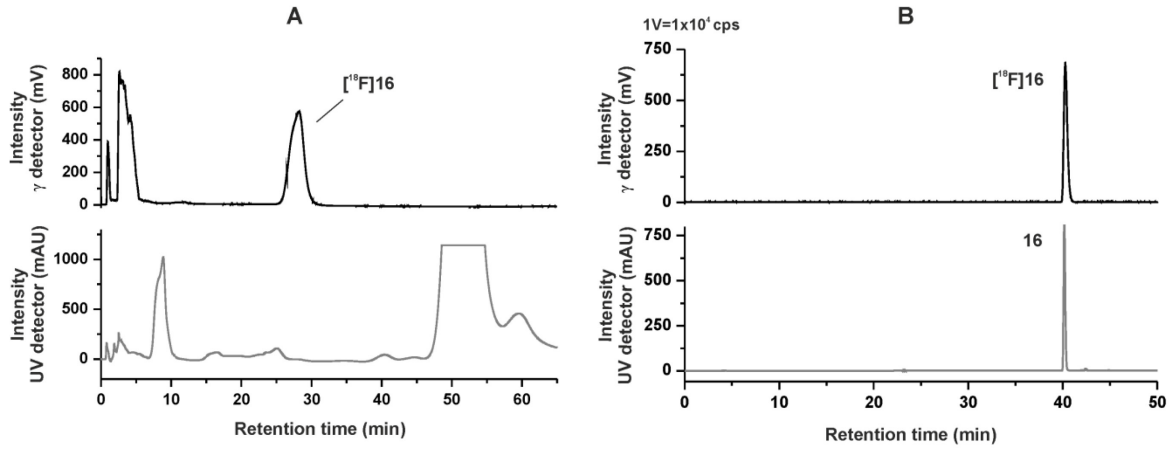

Figure 4. **A**: Semi-preparative radio- and UV-HPLC chromatograms of [^{18}F]**16** (conditions: Reprosil-Pur C18-AQ, 250x10 mm, 62% CH_3CN/20 mM aq NH_4OAc, 4.0 mL/min). **B**: Analytical radio- and UV-HPLC chromatograms of the final product of [^{18}F]**16** spiked with the nonradioactive reference **16** (conditions: Reprosil-Pur C18-AQ, 250x4.6 mm, gradient with eluent mixture of CH_3CN/20 mM aq NH_4OAc, 1.0 mL/min).

2.4. *Metabolism studies of [^{18}F]**16** in vivo*

In vivo metabolism of [^{18}F]**16** was investigated in plasma and brain samples obtained from a single CD-1 mouse at 30 min post injection of the radioligand. Looking to the molecular structure of **16**, several possible metabolic sites are conceivable. The hydrolysis of the amide bond and hydroxylation of aromatic as well as aliphatic carbon atoms are most likely as these are well known metabolic pathways.[47-51] In particular the hydrolysis of the amide function would cleave the molecule resulting in radioactive and nonradioactive metabolites of which only the latter one could be determined in our experiments.

Two different methods were used to analyse the samples: (A) Micellar chromatography (MLC) with a direct injection of the samples and (B) RP-HPLC with injection of extracts obtained after protein precipitation (Figure 5). MLC allows the investigation of the biological samples without eliminating the tissue matrix due to the ability of micellar aggregates to dissolve the proteins and other components. Beside a reduction of analysis time, this method also ensures a quantitative analysis, which is often not given when proteins are precipitated and bound polar or ionic metabolites are not entirely extractable. The radio-MLC method was investigated by Nakao et. al regarding its suitability for plasma metabolite analysis of PET radioligands in clinical use.[52] Recently, our group extended these experiments by using this method to also analyse homogenates of brain samples.[53, 54]

The data obtained with both methods indicated a fast metabolic degradation of the radiotracer. Radio-MLC and radio-RP-HPLC chromatograms of the plasma samples showed only negligible amounts of [^{18}F]**16** and the formation of a main radiometabolite representing more than 85% of total radioactivity (Figure 5). The very fast elution in both chromatography systems argues for a high polarity of the radiometabolite. Moreover, a very low recoveries during the extraction procedure was observed, which is often caused by free [^{18}F]fluoride which partially binds to the precipitated proteins. Therefore, it is assumed that mainly defluorination seems to be responsible for the observed radiometabolite profile of the plasma samples at 30 min p.i. A mechanism for the radiodefluorination of a fluoroethyl chain bound to an aromatic ring was proposed by Lee et al.[47, 49, 51, 55]

Similar radio-chromatographic profiles were observed for the brain samples and no intact radiotracer could be detected (Figure 5). As fluoride is not able to cross the blood-brain barrier considerably, the detected [^{18}F]fluoride might be due to metabolism in the brain or degradation during the working up procedures of the brain samples. The latter can be excluded, because the stability of the radiotracer has been proven under the conditions used for MLC. Drug metabolism in the brain is a phenomenon which is intensively investigated within the last years. In particular the central expression and function of several CYP enzymes emerge evidence of biological relevance. Despite CYP levels in the brain are low with approximately 0.5-2% of those in the liver,[56] it is conceivable that a CYP mediated metabolism in the brain may influence the radiotracer stability because of the negligible injected mass. This observation, was also described many years ago by Coenen et al.[57] who determined a certain level of [^{18}F]fluoride in a brain sample. Welch et al.[58] discussed in the same year this finding and postulated a metabolic process within the brain as a possible explanation.

Since in both, plasma and brain samples, a small amount of a second more lipophilic radiometabolite can be observed, a fast cleavage of the amide function of [^{18}F]**16** caused by hydrolases can additionally be assumed.[50] This would result in the formation of a radioactive

aniline derivative which is supposed to be able to cross the blood-brain barrier and probably also contributes via defluorination to the detected free amount of [^{18}F]fluoride.

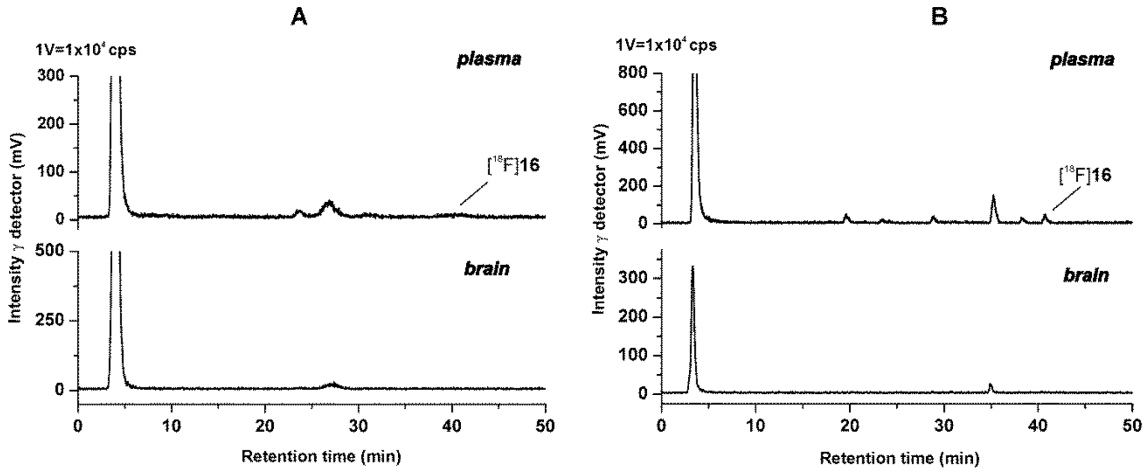

Figure 5. Representative radio chromatograms of a mouse plasma and brain sample of [^{18}F]**16** at 30 min p.i. **A**: Micellar chromatography (conditions: Reprosil-Pur C18-AQ, 250x4.6 mm, gradient: 3-30-3% 1-PrOH/100 mM SDS aq., 10 mM Na_2HPO_4 aq.; flow: 0.75 mL/min). **B**: Reversed phase chromatography (conditions: Reprosil-Pur C18-AQ, 250x4.6 mm, gradient: 10-90-10% ACN/20 mM NH_4OAc aq.; flow 1.0 mL/min).

Finally, the observed strong radiodefluorination of [^{18}F]**16** was rather unexpected, considering that a 2-fluoroethyl-aryl group should be slightly more stable as the corresponding 2-fluoroethoxy-aryl (in this case compound **18**, Scheme 1), which is known to be cleaved quite fast via CYP mediated *O*-dealkylation producing brain penetrant radiometabolites (e.g. fluoroethanol). Moreover, recently we reported on the development of an ^{18}F-labeled radiotracer for imaging the oxytocin receptor,[59] which also contains a fluoroethyl function and did not demonstrate such a fast metabolic degradation. Once more, we resume that the metabolic stability of a particular ^{18}F-bearing functional group considerably depends on the whole molecular structure of the compound. As recently nicely reviewed by Kirchmair et al. the prediction of possible metabolic sites of a compound is rather challenging and needs a close collaboration of experts from different fields.[60]

2.5. Conclusions

In summary, a novel, small series of fluorinated compounds has been developed by modifying the structure of the highly affine and selective $P2Y_1R$ ligand **8**, as potential starting point for the development of an ^{18}F-PET radiotracer for $P2Y_1R$ imaging in the brain. Additionally, the boron-rich derivative **23** was designed by replacing the *p*-(trifluoromethoxy)phenyl subunit with carbaboran as potential therapeutic agent for the use with NCT. Preliminary *in vitro* investigations shown strong antagonist effect for the fluorinated compound **16**. The radioligand [^{18}F]**16** was obtained with high radiochemical purity, yield and molar activities. First in vivo experiment performed with a CD-1 mouse revealed a fast metabolism with nearly no intact [^{18}F]**16** to be detected at 30 minutes post injection in plasma and brain samples. Further research will focus on the establishment of an in vitro competitive radioligand binding assay in our labs but also on the introduction of the $^{18}F^{-}$-label at a

different position of the molecule e.g. 2-pyridine position which might hinder the formation of brain penetrant radiometabolites.

3 Experimental

3.2 Chemistry

3.2.1 General methods

Unless otherwise noted, moisture sensitive reactions were conducted under dry nitrogen or argon. All chemicals and reagents were purchased from commercially available sources and used without further purification. Thin layer chromatography (TLC): Silica gel 60 F254 plates (Merck KGaA, Darmstadt, Germany). Flash chromatography (fc): Silica gel 60, 40-64 µm (Merck). Room temperature (rt.) was 21 °C. MS: MAT GCQ (Thermo Finnigan MAT GmbH, Bremen, Germany). ^{1}H, ^{13}C and ^{19}F NMR spectra were recorded on VARIAN "MERCURY plus" (300 MHz for ^{1}H NMR, 75 MHz for ^{13}C NMR, 282 MHz for ^{19}F NMR) and VARIAN "MERCURY plus" and BRUKER DRX-400 (400 MHz for ^{1}H NMR, 100 MHz for ^{13}C NMR, 377 MHz for ^{19}F NMR); δ in ppm related to tetramethylsilane; coupling constants (J) are given with 0.1 Hz resolution. Multiplicities of NMR signals are indicated as follows: s (singlet), d (doublet), t (triplet), m (multiplet), dd (doublet of doublets), dt (doublet of triplets). ESI/Ion trap mass spectra (LRMS) were recorded with a Bruker Esquire 3000 plus instrument (Billerica, MA, USA). High resolution mass spectra were recorded on a FT-ICR APEX II spectrometer (Bruker Daltonics; Bruker Corporation, Billerica, MA, USA) using electrospray ionization (ESI) in positive ion mode.

3.2.2 Procedures and compound characterization

General procedure A 2-halo-3-nitropyridine (1 eq, 7.3 mmol) in DMF (6 mL) was treated with 2-isopropylphenol (1 eq, 7.3 mmol) and Cs_2CO_3 (1.5 eq, 10.9 mmol). The mixture was heated at 70 °C for 14 h. The reaction was cooled to room temperature, and DMF was evaporated. The residue was taken up in EA (20 mL) and was washed with 5% LiCl aq. sol. (3 × 7 mL) and brine (3 × 7 mL). Drying ($MgSO_4$) and removal of solvent afforded a brown solid which was recrystallized from ethanol to afford the corresponding ether as yellow needles.

General procedure B A solution of nitro compound (1 eq, 7.4 mmol) in MeOH/THF (1:4, 16 mL) was reduced under H_2 atmosphere (1 atm) in presence of Pd/C (10 mol%) overnight at room temperature. The reaction mixture was filtered over Celite and concentrated to afford a white solid which was recrystallized from EA to afford corresponding amine as a white powder.

General procedure C A solution of DCM (10 mL) containing Et_3N (3 eq, 13 mmol) was added to a solution of the amine (1 eq, 4.4 mmol) and diphosgene (0.8 eq, 3.5 mmol) in DCM (20 mL) at 0 °C, dropwise. After the addition was completed, the resulting mixture was stirred at 0 °C for 45 min and an additional 2 hours at room temperature then washed with 0.5 M HCl (3 × 20 mL), 1 N NaOH (2 × 10 mL), and brine. Drying ($MgSO_4$) and removal of solvent afforded the corresponding isocyanate as a yellow solid. This material was used for the subsequent reaction without further purification

General procedure D Substituted aniline (1 eq, 0.2 mmol) was added to a solution of isocyanate (1 eq, 0.2 mmol) in toluene (1 mL) under argon. The resulting mixture was stirred at 80 °C for 1.5 h. The solvent was removed by rotary evaporation, and the crude product was purified by flash chromatography the diaryl urea as colorless solid.

2-(2-(*tert*-Butyl)phenoxy)pyridin-3-amine (**12**): colorless solid, 55% yield over 2 steps; TLC (silica gel, EA/IH, 2:8): $R_f = 0.55$.

^{1}H NMR (400 MHz, $CDCl_3$): $\delta = 7.59$ (dd, $J = 4.9$, 1.7 Hz, 1H), 7.44 (dd, $J = 7.8$, 1.8 Hz, 1H), 7.25 – 7.16 (td, J = 7.6, 1.5 Hz, 1H), 7.11 (td, $J = 7.6$, 1.5 Hz, 1H), 7.04 (dd, $J = 7.6$, 1.6 Hz, 1H), 6.93 (dd, $J = 7.9$, 1.5 Hz, 1H), 6.83 (dd, $J = 7.6$, 4.9 Hz, 1H), 3.95 (s, 2H), 1.42 (s, 9H).

^{13}C NMR (100 MHz, $CDCl_3$): δ = 152.9, 152.0, 141.1, 136.2, 132.2, 127.4, 127.0, 124.3, 122.6, 122.0, 119.2, 30.5 (3C).

1-(2-(2-(t*ert*-Butyl)phenoxy)pyridin-3-yl)-3-(4-(trifluoromethoxy)phenyl)urea (**8**) General Procedure D (colorless solid, 95%)

M. p. = 152 °C.

TLC (silica gel, EA/IH, 3:7): $R_f = 0.50$.

^{1}H NMR (400 MHz, $CDCl_3$): $\delta = 8.53$ (dd, $J = 8.0$, 1.7 Hz, 1H), 7.79 (dd, $J = 4.9$, 1.7 Hz, 1H), 7.49 (s, 1H), 7.46 – 7.37 (m, 1H), 7.32 (s, 1H), 7.30 – 7.22 (m, 2H), 7.22 – 7.05 (m, 4H), 6.94 (dd, $J = 7.9$, 4.9 Hz, 1H), 6.87 – 6.76 (m, 1H), 1.29 (s, 9H).

^{13}C NMR (100 MHz, $CDCl_3$): δ = 153.0, 152.9, 152.3, 145.8, 141.5, 140.6, 136.2, 127.8, 127.7, 127.3, 125.2, 124.2, 123.1, 122.7, 122.2, 122.1 (2C), 119.1 (2C), 34.75, 30.63 (3C).

^{19}F NMR (282 MHz, $CDCl_3$): $\delta = -58.56$.

HRFTMS (ESI+): m/z = 446.1686 (calcd. 446.1686 for $C_{23}H_{23}F_3N_3O_3$ $[M+H]^+$).

1-(2-(2-(*tert*-Butyl)phenoxy)pyridin-3-yl)-3-(4-(2-hydroxyethyl)phenyl)urea (**14**) General Procedure D (colorless solid, 72% yield)

M. p. = 192 °C.

TLC (silica gel, EA/IH, 1:1): $R_f = 0.38$.

^{1}H NMR (400 MHz, $CDCl_3$): $\delta = 8.54$ (dd, $J = 8.0$, 1.7 Hz, 1H), 7.66 (dd, $J = 4.9$, 1.7 Hz, 1H), 7.39 (dd, $J = 7.6$, 1.9 Hz, 1H), 7.34 – 7.22 (m, 2H), 7.15 – 7.07 (m, 4H), 6.92 (dd, J = 8.0, 4.9 Hz, 1H), 6.78 (dd, $J = 7.7$, 1.7 Hz, 1H), 3.71 (t, $J = 6.7$ Hz, 2H), 2.73 (t, $J = 6.7$ Hz, 2H), 1.30 (s, 9H).

^{13}C NMR (100 MHz, $CDCl_3$): δ = 153.7, 153.6, 152.7, 141.6, 139.4, 136.8, 136.7, 133.9, 129.6, 127.5, 127.3 (2C), 127.2, 125.1, 124.9, 123.0, 120.3, 119.0, 63.3, 38.4, 34.6, 30.5 (3C).

HRFTMS (ESI+): m/z = 406.2125 (calcd. 406.2125 for $C_{24}H_{28}N_3O_3$ $[M+H]^+$).

4-(3-(2-(2-(*tert*-Butyl)phenoxy)pyridin-3-yl)ureido)phenethyl 4-methylbenzenesulfonate (**15**) General Procedure E (colorless solid, quantitative)

M. p. = 190 °C.

TLC (silica gel, EA/IH, 1:1): $R_f = 0.80$.

^{1}H NMR (400 MHz, $CDCl_3$): $\delta = 8.58$ (dd, $J = 8.0$, 1.7 Hz, 1H), 7.78 (dd, $J = 4.9$, 1.7 Hz, 1H), 7.67 (d, $J = 8.3$ Hz, 2H), 7.41 (dd, $J = 7.7$, 1.9 Hz, 1H), 7.39 (s, 1H) 7.28 (s, 1H), 7.21 (d, $J = 8.3$ Hz, 2H) 7.20 – 7.10 (m, 2H), 7.03 (d, $J = 8.4$ Hz, 2H), 6.96 (dd, $J = 8.0$, 4.9 Hz, 1H), 6.91 (s, 1H), 6.82 (dd, $J = 7.8$, 1.6 Hz, 1H), 4.15 (t, $J = 7.0$ Hz, 2H), 2.88 (t, $J = 7.0$ Hz, 2H), 2.43 (s, 3H), 1.28 (s, 9H).

^{13}C NMR (100 MHz, $CDCl_3$): δ = 153.0, 152.7, 152.4, 144.9, 141.5, 140.3, 136.4, 133.0, 132.9, 130.0, 129.9, 127.9 (2C), 127.6, 127.4, 127.2, 125.1, 124.5, 123.2, 122.2, 119.1, 77.5, 77.1, 76.8, 70.5, 34.8, 34.7, 30.6 (3C), 21.7.
FTMS (ESI+): *m/z* = 560.3 (calcd. 560.2 for $C_{31}H_{34}N_3O_5S$ $[M+H]^+$).
1-(2-(2-(*tert*-Butyl)phenoxy)pyridin-3-yl)-3-(4-(2-fluoroethyl)phenyl)urea (16) General Procedure (colorless solid, 62%)
M. p. = 135 °C.
TLC (silica gel, EA/IH, 2:8): R_f = 0.35.
^{1}H NMR (400 MHz, $CDCl_3$): δ = 8.61 (dd, *J* = 7.9, 1.7 Hz, 1H), 7.79 (dd, *J* = 4.9, 1.7 Hz, 1H), 7.42 (dd, *J* = 7.7, 1.9 Hz, 1H), 7.36 – 7.26 (m, 3H), 7.24 – 7.09 (m, 4H), 6.99 (dd, *J* = 8.0, 4.9 Hz, 1H), 6.84 (dd, *J* = 7.8, 1.6 Hz, 1H), 6.59 (s, 1H), 4.58 (dt, *J* = 47.0, 6.5 Hz, 2H), 2.96 (dt, *J* = 23.7, 6.4 Hz, 2H), 1.28 (s, 9H).
^{13}C NMR (100 MHz, $CDCl_3$): δ = 153.1, 152.6, 152.5, 140.4, 135.9, 134.6, 130.4, 127.7, 127.5, 127.3, 125.1, 124.6, 123.2 (3C), 119.2 (2C), 85.1, 82.9, 36.6, 36.4, 30.7 (3C)
^{19}F NMR (282 MHz, $CDCl_3$): δ = –216.10.
HRFTMS (ESI+): *m/z* = 408.2082 (calcd. 408.2082 for $C_{24}H_{27}FN_3O_2$ $[M+H]^+$).

1-(2-(2-(*tert*-Butyl)phenoxy)pyridin-3-yl)-3-(4-hydroxyphenyl)urea (**17**) General Procedure (colorless solid, 85%).
M. p. = 213 °C.
TLC (silica gel, EA/IH, 2:8): R_f = 0.10.
^{1}H NMR (400 MHz, $CDCl_3$): δ = 8.55 (dd, *J* = 8.0, 1.7 Hz, 1H), 7.66 (dd, *J* = 4.9, 1.7 Hz, 1H), 7.47 – 7.37 (m, 2H), 7.26 – 7.07 (m, 4H), 6.97 (dd, *J* = 8.0, 4.9 Hz, 1H), 6.80 (dd, *J* = 7.8, 1.5 Hz, 1H), 6.78 – 6.70 (m, 2H), 1.32 (s, 9H).
^{13}C NMR (100 MHz, $CDCl_3$): δ = 154.5, 153.0, 152.9, 141.7, 139.2 (2C), 127.6 (2C), 127.5 (2C), 127.2, 125.5, 125.0, 123.1 (2C), 119.1, 115.9 (2C), 34.7, 30.5 (3C).
HRFTMS (ESI+): *m/z* = 378.1812 (calcd. 378.1812 for $C_{22}H_{24}N_3O_3$ $[M+H]^+$).
1-(2-(2-(*tert*-Butyl)phenoxy)pyridin-3-yl)-3-(4-(2,2,2-trifluoroethoxy)phenyl)urea (**19**) CF_3CH_2OTs (134 mg, 4 eq, 0.52 mmol) was reacted with **17** (50 mg, 1 eq, 0.13 mmol) in presence of K_2CO_3 (55 mg, 3 eq, 0.40 mmol) in MeCN (5 mL) at 82 °C under argon for 16 hours. Saturated aqueous $NaHCO_3$ solution (10 mL) was added and the mixture was washed with EA (3 x 10 mL). The combined EA fractions were washed with H_2O (1 x 10 mL), saturated aqueous $NaHCO_3$ (1 x 10) mL and dried over $MgSO_4$. The solvent was removed by rotary evaporation and the remaining residue was purified by flash chromatography (silica, EA/IH 1:9) to give **19** (29 mg, 0.06 mmol, 48%) as colorless solid.
M. p. = 165 °C.
TLC (silica gel, EA/IH, 2:8) R_f = 0.55.
^{1}H NMR (400 MHz, $CDCl_3$): δ = 8.60 (d, *J* = 7.5 Hz, 1H), 7.79 (s, 1H), 7.41 (d, *J* = 7.4 Hz, 1H), 7.37 – 7.07 (m, 5H), 7.06 – 6.54 (m, 4H), 4.29 (q, *J* = 8.1 Hz, 2H), 1.26 (s, 9H).
^{13}C NMR (100 MHz, $CDCl_3$): δ = 155.4 (2C), 152.6, 152.4, 141.4, 140.3, 131.5, 127.6 (2C), 127.4, 127.3, 125.5 (2C), 125.0, 124.6, 124.6 (m, 1C), 123.1, 119.2, 116.2 (2C), 66.3 (d, J = 44.8 Hz, 1C), 34.7, 30.6 (3C).
^{19}F NMR (282 MHz, $CDCl_3$): δ = –74.39.
HRFTMS (ESI+): *m/z* = 482.1662 (calcd. 482.1662for $C_{24}H_{25}F_3N_3O_3$ $[M+H]^+$).

1-(2-(2-(tert-Butyl)phenoxy)pyridin-3-yl)-3-(4-(2-fluoroethoxy)phenyl)urea (**18**) was obtained by the same procedure as compound **19** with $Br(CH_2)_2F$ as alkylating reagent. (colorless solid, 82%)
M. p. = 179 °C.
TLC (silica gel, EA/IH, 2:8): $R_f = 0.13$.
^{1}H NMR (400 MHz, $CDCl_3$): $\delta = 8.60$ (dd, $J = 8.0$, 1.7 Hz, 1H), 7.76 (dd, $J = 4.9$, 1.7 Hz, 1H), 7.41 (d, $J = 1.6$ Hz, 1H), 7.40 (dd, $J = 7.7$, 1.8 Hz, 1H), 7.21 (d, $J = 8.9$ Hz, 2H), 7.14 (tdd, $J = 8.9$, 6.2, 2.4 Hz, 2H), 6.95 (dd, $J = 7.9$, 4.9 Hz, 2H), 6.83 (d, $J = 8.8$ Hz, 2H), 6.85 – 6.79 (m, 1H), 4.84 – 4.57 (m, 2H), 4.24 – 4.03 (m, 2H), 1.25 (s, 9H).
^{13}C NMR (100 MHz, $CDCl_3$): δ = 156.5, 153.9, 152.6, 152.5, 141.4, 140.1, 130.4, 127.7, 127.3, 127.1, 125.6, 124.9, 124.7, 123.1, 119.1, 115.7, 83.1, 80.8, 81.9 (d, $J = 171.0$ Hz, 1C), 67.5 (d, $J = 20.5$ Hz, 1C). 34.6, 30.6 (3C).
^{19}F NMR (282 MHz, $CDCl_3$): $\delta = -224.30$.
HRFTMS (ESI+): m/z = 424.2031 (calcd. 424.2031 for $C_{24}H_{27}FN_3O_3$ $[M+H]^+$).
N-(2-(2-(*tert*-Butyl)phenoxy)pyridin-3-yl)-4-(trifluoromethyl)thiazol-2-amine (**20**)
A mixture of **12** (500 mg, 1 eq, 2.06 mmol) and benzoyl isothiocyanate (306 µL, 1.1 eq, 2.27 mmol) was refluxed in 10 mL DCM for 2 h. Elimination of the solvent under reduced pressure afforded a thick yellowish oil which was redissolved in a 2M LiOH/MeOH (3:1, 15 mL) and warmed at 50 °C for 2 h. H_2O (20 mL) and EA (20 mL) were added under stirring and the phases were separated in a separatory funnel. The organic phase was washed with aqueous saturated $NaHCO_3$ and NaCl solutions, dried over $MgSO_4$ and concentrated under reduced pressure to give the corresponding thiourea as tan solid, which was used without purification in the next step. 3-bromo-1,1,1-trifluoropropan-2-one (221 µL, 1.3 eq, 21.5 mmol) and 2,6-lutidine (287 µL, 2 eq, 3.3 mmol) were added to the above obtained thiourea intermediate (500 mg, 1 eq, 1.65 mmol) and in EtOH (15 mL) and the mixture was refluxed under argon for 24 h. The solvent was evaporated, 20 mL 2M HCl was added and the mixture was washed with EA (2 x 15 mL). The combined organic phases were washed 1 x 15 mL $NaHCO_3$ and 1 x 10 mL NaCl aqueous saturated solutions, dried over $MgSO_4$ and concentrated under reduced pressure to give a yellow solid which was further washed 3 x 10 mL hexane. Upon solvent evaporation under reduced pressure **20** (650 mg, 82% over 3 steps) was obtained as a light grey solid.
M. p. = 65 °C.
TLC (silica gel, EA/IH, 1:9): $R_f = 0.55$.
^{1}H NMR (400 MHz, $CDCl_3$): $\delta = 8.60$ (dd, $J = 7.9$, 1.6 Hz, 1H), 7.83 (dd, $J = 4.9$, 1.7 Hz, 2H), 7.48 (dd, $J = 7.7$, 1.9 Hz, 1H), 7.33 – 7.14 (m, 3H), 7.07 (dd, $J = 7.9$, 4.9 Hz, 1H), 6.94 (dd, $J = 7.8$, 1.6 Hz, 1H), 1.40 (s, 9H).
^{13}C NMR (100 MHz, $CDCl_3$): δ = 164.2, 152.2, 152.1, 141.6, 140.1, 127.7, 127.3, 125.5, 125.3 (2C), 125.0, 123.3, 119.1, 110.9 (dd, $J = 7.9$, 3.9 Hz), 34.8, 30.8 (9C).
^{19}F NMR (282 MHz, $CDCl_3$): $\delta = -65.51$.
N-(2-(2-(*tert*-Butyl)phenoxy)pyridin-3-yl)-5-(6-fluoropyridin-3-yl)-4-(trifluoromethyl)thiazol-2-amine (**21**). To a solution of **20** (200 mg, 1 eq, 0.52 mmol) in 10 mL AcOH/THF (1:5) at 0 °C, NBS (103 mg, 1.1 eq, 0.58 mmol) was added and the reaction was stirred for 2 h at 0 °C. EA (15 mL) was added and the organic solution was washed with 15 mL H_2O, concentrated aqueous $NaHCO_3$ and NaCl solutions dried over $MgSO_4$ and

concentrated under reduced pressure. The resulting solid was purified by flash chromatography (silica, EA/IH, 1:18) to give the corresponding 5-bromo-2-aminothiazole intermediate (198 mg, 82%) as colorless tan solid. Under argon, the so obtained 5-bromo-2-aminothiazole intermediate (50 mg, 1 eq, 0.11 mmol), 2-fluoropyridin-5-boronic acid (23 mg, 1.5 eq, 0.17 mmol), $Pd(PPh_3)_4$ (13 mg, 0.1 eq, 0.01 mmol) and Na_2CO_3 (34 mg, 3 eq, 0.33 mmol) were added to 5 mL toluene/EtOH (2:1) at rt and the whole was refluxed (95 °C) overnight. The solvent was eliminated by rotary evaporation and the resulting mass was subject of purification by flash chromatography (EA/IH, 1:39). Compound **21** (38 mg, 0.8 mmol, 78%) was obtained as colorless solid

M. p. = 197 °C.

TLC (silica gel, EA/IH, 1:9): $R_f = 0.24$.

^{1}H NMR (400 MHz, $CDCl_3$): δ = 8.56 (dd, J = 7.9, 1.6 Hz, 1H), 8.32 (d, J = 2.3 Hz, 1H), 7.91 – 7.84 (m, 3H), 7.48 (dd, J = 7.7, 1.8 Hz, 1H), 7.31 – 7.15 (m, 2H), 7.08 (dd, J = 7.9, 5.0 Hz, 1H), 7.03 (dd, J = 8.4, 3.0 Hz, 1H), 6.94 (dd, J = 7.8, 1.4 Hz, 1H), 1.39 (s, 9H).

^{13}C NMR (100 MHz, $CDCl_3$): δ = 165.1, 162.7, 162.3, 152.3, 152.1, 148.5, 148.3, 142.6 (d, J = 1.4 Hz), 142.5 (d, J = 1.4 Hz), 141.6, 140.5, 127.8, 127.3, 125.4, 125.2, 125.1, 123.3 (d, J = 5.9 Hz), 119.1, 109.8, 109.6, 34.8, 30.8 (3C).

^{19}F NMR (282 MHz, $CDCl_3$): δ = –60.40 (3F), –66.73 (1F).

HRFTMS (ESI+): m/z = 489.1367 (calcd. 489.1367 for $C_{24}H_{21}F_4N_4OS$ $[M+H]^+$).

1-(1,2-*closo*-dodecaborane)-3-(2-(2-(*tert*-butyl)phenoxy)-6-fluoropyridin-3-yl)urea (**23**) was obtained by *General Procedure D* with a reaction time of 24 h (colorless solid, 22% yield).

^{1}H NMR (400 MHz, $CDCl_3$): δ = 8.37 (dd, J = 8.0, 1.7 Hz, 1H), 7.84 (dd, J = 4.9, 1.7 Hz, 1H), 7.49 – 7.45 (m, 1H), 7.32 (s, 1H), 7.25 – 7.18 (m, 2H), 6.99 (dd, J = 8.0, J = 4.9 Hz, 1H), 6.84 (dd, J = 7.9, 4.9 Hz, 1H), 6.77 – 6.73 (m, 1H), 4.71 (s, CH-cluster, 1H), 4.0 – 1.5 (m, BH-cluster, 10H) 1.36 (s, 9H).

^{13}C NMR (100 MHz, $CDCl_3$): δ = 153.0, 152.3, 151.6, 145.8, 141.5, 141.3, 127.9, 127.8, 127.4, 125.4 (2C), 123.2, 119.0, 61.4, 34.7, 30.6 (3C).

HRFTMS (ESI+): m/z+1 = 451.3164 (calcd. 451.3119 for $C_{18}H_2B_{10}N_3NaO_2$ $[M+Na]^+$).

3.3 Radiochemistry

3.3.1 General

No-carrier-added [^{18}F]fluoride was produced via the [^{18}O(p,n)^{18}F] nuclear reaction by irradiation of an [^{18}O]H_2O target (Hyox 18 enriched water, Rotem Industries Ltd, Israel) on a Cyclone 18/9 (iba RadioPharma Solutions, Belgium) with fixed energy proton beam using Nirta [^{18}F]fluoride XL target.

Radio thin layer chromatography (radio-TLC) was performed on silica gel (Polygram® SIL G/UV_{254}) pre-coated plates with a mixture of EA/IH 1:1 (v/v) as eluent. The plates were exposed to storage phosphor screens (BAS-TR2025, FUJIFILM Co., Tokyo, Japan) and recorded using a bio-imaging analyser system (BAS-1800 II, FUJIFILM). Images were evaluated with the BASReader and AIDA 2.31 software (raytest Isotopenmessgeräte GmbH, Straubenhardt, Germany).

Analytical chromatographic separations were performed on a JASCO LC-2000 system, incorporating a PU-2080*Plus* pump, AS-2055*Plus* auto injector (100 µL sample loop), and a UV-2070*Plus* detector coupled with a gamma radioactivity HPLC detector (Gabi Star, raytest Isotopenmessgeräte GmbH). Data analysis was performed with the Galaxie chromatography software (Agilent Technologies) using the chromatograms obtained at 254 nm. A Reprosil-Pur C18-AQ column (250 x 4.6 mm; 5 µm; Dr. Maisch HPLC GmbH; Germany) with ACN/20 mM NH_4OAc aq. (pH 6.8) as eluent mixture and a flow of 1.0 mL/min was used (gradient: eluent A 10% ACN/20 mM NH_4OAc aq.; eluent B 90% ACN/20 mM NH_4OAc aq.; 0–10' 100% A, 10–40' up to 100% B, 40–50' 100% B , 50–51 up to 100% A, 51–60' 100% A).

Semi-preparative HPLC separations were performed on a JASCO LC-2000 system, incorporating a PU-2080-20 pump, an UV/VIS-2075 detector coupled with a gamma radioactivity HPLC detector whose measurement geometry was slightly modified (Gabi Star, raytest Isotopenmessgeräte GmbH) and a fraction collector (Advantec CHF-122SC). A Reprosil-Pur C18-AQ column (150 x 10 mm) coupled with a precolumn (50 x 10 mm; 10 µm; Dr. Maisch HPLC GmbH; Germany) with 62% ACN/20 mM $NH_4OAc_{aq.}$ (pH 6.8) as eluent at a flow of 4.0 mL/min were used.

The ammonium acetate and the SDS concentrations stated as 20 mM NH_4OAc aq. and 100 mM aq., respectively, correspond to the concentration in the aqueous component of an eluent mixture.

3.3.2 Radiosynthesis

No carrier added [^{18}F]fluoride (100 - 500 µL) was transferred into a 4 mL V vial and $TBAHCO_3$ (20 µL of a 0.075 M aqueous solution from ABX advanced biochemical compounds, Radeberg, Germany) in 1 mL ACN was added. The aqueous [^{18}F]fluoride was azeotropically dried under vacuum and nitrogen flow within 7-10 min using a single mode microwave (75 W, at 50–60 °C, power cycling mode). Two aliquots of anhydrous ACN (2 x 1.0 mL) were added during the drying procedure and the final [^{18}F]TBAF was dissolved in 500 µL of anhydrous *tert*-BuOH ready for labelling. Thereafter, a solution of 1.8−2.0 mg of precursor in 300 µL of anhydrous *tert*-BuOH was added, and the ^{18}F-labelling was performed under thermal heating at 90 °C for 10 min. To analyse the reaction mixture and to determine labelling efficiencies, samples were taken for radio-HPLC and radio-TLC. Moreover, the stability of the tosylate precursor was investigated under the labelling conditions by using UV-HPLC analysis.

After cooling, 2.0 mL of a mixture of ACN/water (35/75 v/v) was added and the solution was applied to an isocratic semi-preparative RP-HPLC system for isolation of [^{18}F]**16**. The collected radiotracer fraction was diluted with 40 mL of H_2O to perform final purification by sorption on a preconditioned Sep-Pak® C18 light cartridge (Waters, Milford, MA, USA) and successive elution with 0.75 mL of ethanol. The solvent was reduced under a gentle argon stream at 70 °C and the desired radiotracer formulated in sterile isotonic saline containing 10% EtOH (v/v). The identity and radiochemical purity of [^{18}F]**16** was confirmed by radio-HPLC and radio-TLC. Specific activity was determined on the basis of a UV/mass calibration curve carried out under isocratic HPLC conditions (62% ACN/20 mM $NH_4OAc_{aq.}$, pH 6.8) using chromatograms obtained at 260 nm.

3.4 Metabolism studies

Blood samples of mouse were taken at 30 min after intravenous injection of ~65 MBq of [^{18}F]**16** (n = 1). Plasma was obtained by centrifugation of blood at 12,000 rpm at 4 °C for 10 min.

Method (A) - MLC: For preparation of the MLC injection samples, mouse plasma (20 – 50 µL, 30 min p.i.) was dissolved in 100 – 300 µL of 100 mM aqueous SDS. Homogenized brain material (200 µL, 30 min p.i.) was dissolved in 400 µL of 200 mM aqueous SDS, stirred at 75 °C for 5 minutes and injected into the MLC system after cooling to room temperature. To proof the integrity of the radiotracer under this conditions, 50 kBq of the radiotracer were stirred at 75 °C for 5 min in 500 µl of 200 mM aqueous SDS and analysed via MLC. The MLC system was built up of a JASCO PU-980 pump, an AS-2055*Plus* auto injector with a 2000 µL sample loop, and a UV-1575 detector coupled with a gamma radioactivity HPLC detector (Gabi Star, raytest Isotopenmessgeräte GmbH). Data analysis was performed with the Galaxie chromatography software (Agilent Technologies). A Reprosil-Pur C18-AQ column (250 x 4.6 mm, particle size: 10 µm) coupled with a pre-column of 10 mm length was used. Separations were performed by using an eluent mixture of 1-PrOH/100 mM aqueous SDS/10mM Na_2HPO_4 aq. in gradient mode (0 – 15' at 3% 1-PrOH, 15 – 30' up to 30% 1-PrOH, 30 – 45' at 30% 1-PrOH, 45 – 50' up to 3% 1-PrOH; 50 – 60' at 3% 1-PrOH/ 100 mM SDS aq., 10 mM Na_2HPO_4 aq.) at a flow rate of 0.75 mL/min.

Method (B) - RP-HPLC: For protein precipitation and extraction two different solvent systems were tested by adding an ice-cold mixture of (i) acetone/water (4/1; v/v) and (ii) MeOH/water (9/1; v/v) in a ratio of 4 : 1 of solvent to plasma or brain homogenate, respectively. The samples were vortexed for 2 min, equilibrated on ice for 15 min, and centrifuged for 5 min at 10,000 rpm. The precipitates were washed with 200 µL of the solvent mixture and subjected to the same procedure. The combined supernatants (total volume between 1.0 –1.5 mL) were concentrated at 65 °C under nitrogen flow to a final volume of approximately 100 µL and analysed by analytical radio-HPLC. To determine the percentage of radioactivity in the supernatants compared to total activity, aliquots of each step as well as the precipitates were quantified by γ counting. Using the acetone/water system, the obtained recoveries were lower with 44% for plasma and 26% for the brain homogenate compared to the MeOH/water system with 70% and 57%, respectively. To analyse the worked-up samples, the same HPLC method was used as described in the radiochemistry part.

Supplementary Materials: ^{1}H NMR spectra of target compounds and crystallographic data.

Acknowledgments: We thank the staff of the Institute of Analytical Chemistry, Department of Chemistry and Mineralogy of the University of Leipzig, for the MS and NMR spectra.

Author Contributions: Rareş-Petru Moldovan conceived and performed the chemical syntheses, Wilma Neumann and Evamarie Hey-Hawkins were involved in the synthesis of the carbaborane derivative, Barbara Wenzel and Rodrigo Teodoro planned and performed the radiosynthesis, and metabolic stability studies, Sladjana Dukic-Stefanovic, Winnie Deuther-Conrad, Ute Krügel and Peter Brust planned and performed the biological experiments. All coauthors analyzed the data and wrote and accepted the manuscript.

Conflicts of Interest: The authors declare no conflict of interest.

Funding: No funding source

References

1. Burnstock, G. Introduction to purinergic signalling in the brain. In *Glioma Signaling*, Barańska, J., Ed. Springer Netherlands: Dordrecht, 2013; pp 1-12.
2. Abbracchio, M. P.; Burnstock, G.; Verkhratsky, A.; Zimmermann, H. Purinergic signalling in the nervous system: an overview. *Trends Neurosci.* **2009,** 32, 19-29.
3. Burnstock, G. Introductory overview of purinergic signalling. *Front. Biosci. (Elite Ed.)* **2011,** 3, 896-900.
4. Norenberg, W.; Illes, P. Neuronal P2X receptors: localisation and functional properties. *Naunyn-Schmiedeberg's archives of pharmacology* **2000,** 362, 324-39.
5. von Kugelgen, I.; Hoffmann, K. Pharmacology and structure of P2Y receptors. *Neuropharmacology* **2016,** 104, 50-61.
6. North, R. A. Molecular physiology of P2X receptors. *Physiol. Rev.* **2002,** 82, 1013-1067.
7. Kaczmarek-Hájek, K.; Lörinczi, É.; Hausmann, R.; Nicke, A. Molecular and functional properties of P2X receptors—recent progress and persisting challenges. *Purinergic Signalling* **2012,** 8, 375-417.
8. Dal Ben, D.; Buccioni, M.; Lambertucci, C.; Marucci, G.; Thomas, A.; Volpini, R. Purinergic P2X receptors: structural models and analysis of ligand-target interaction. *Eur. J. Med. Chem.* **2015,** 89, 561-580.
9. <http://www.nobelprize.org/nobel_prizes/chemistry/laureates/2012/press.html> , T. N. P. i. C.-P. R. N. o. N. M. A. W. N.
10. Jacobson, K. A.; Muller, C. E. Medicinal chemistry of adenosine, P2Y and P2X receptors. *Neuropharmacol.* **2016,** 104, 31-49.
11. Rodrigues, R. J.; Tomé, A. R.; Cunha, R. A. ATP as a multi-target danger signal in the brain. *Front. Neurosci.* **2015,** 9.
12. Krugel, U. Purinergic receptors in psychiatric disorders. *Neuropharmacology* **2016,** 104, 212-225.
13. Conroy, S.; Kindon, N.; Kellam, B.; Stocks, M. J. Drug-like antagonists of P2Y receptors—from lead identification to drug development. *J. Med. Chem.* **2016**, In Press.
14. Baranska, J.; Czajkowski, R.; Pomorski, P. P2Y1 Receptors - Properties and functional activities. *Adv. Exp. Med. Biol.* **2017**, 1-19.
15. Boeynaems, J.-M.; Robaye, B.; Janssens, R.; Suarez-Huerta, N.; Communi, D. Overview of P2Y receptors as therapeutic targets. *Drug Dev. Res.* **2001,** 52, 187-189.
16. Rassendren, F.; Audinat, E. Purinergic signaling in epilepsy. *J. Neurosci. Res.* **2016,** 94, 781-793.
17. Di Virgilio, F.; Vuerich, M. Purinergic signaling in the immune system. *Auton. Neurosci.* **2015,** 191, 117-23.
18. Di Virgilio, F. Purines, purinergic receptors, and cancer. *Cancer. Res.* **2012,** 72, 5441-5447.
19. Djerada, Z.; Feliu, C.; Richard, V.; Millart, H. Current knowledge on the role of P2Y receptors in cardioprotection against ischemia-reperfusion. *Pharmacol. Res.* **2016**, In Press.
20. Jacobson, K. A.; Deflorian, F.; Mishra, S.; Costanzi, S. Pharmacochemistry of the platelet purinergic receptors. *Purinergic Signal.* **2011,** 7, 305-324.
21. Felix, R. A.; Martin, S.; Pinion, S.; Crawford, D. J. Development of a comprehensive set of P2 receptor pharmacological research compounds. *Purinergic Signal.* **2012,** 8, 101-112.
22. Houston, D.; Costanzi, S.; Jacobson, K. A.; Harden, T. K. Development of selective high affinity antagonists, agonists, and radioligands for the $P2Y_1$ receptor. *Comb. Chem. High throughput Screen.* **2008,** 11, 410-419.
23. Bourdon, D. M.; Mahanty, S. K.; Jacobson, K. A.; Boyer, J. L.; Harden, T. K. (*N*)-methanocarba-2MeSADP (MRS2365) is a subtype-specific agonist that induces rapid desensitization of the $P2Y_1$ receptor of human platelets. *J. Thromb. Haemost.* **2006,** 4, 861-868.

24. Lipinski, C. A. Drug-like properties and the causes of poor solubility and poor permeability. *J. Pharmacol. Toxicol. Methods* **2000,** 44, 235-249.
25. Di, L.; Kerns, E. H.; Carter, G. T. Drug-like property concepts in pharmaceutical design. *Curr. Pharm. Des.* **2009,** 15, 2184-2194.
26. Brust, P.; van den Hoff, J.; Steinbach, J. Development of [^{18}F]-labeled radiotracers for neuroreceptor imaging with positron emission tomography. *Neurosci. Bull.* **2014,** 30, 777-811.
27. Thalji, R. K.; Aiyar, N.; Davenport, E. A.; Erhardt, J. A.; Kallal, L. A.; Morrow, D. M.; Senadhi, S.; Burns-Kurtis, C. L.; Marino, J. P., Jr. Benzofuran-substituted urea derivatives as novel P2Y$_1$ receptor antagonists. *Bioorg. Med. Chem. Lett.* **2010,** 20, 4104-4107.
28. Costanzi, S.; Santhosh Kumar, T.; Balasubramanian, R.; Kendall Harden, T.; Jacobson, K. A. Virtual screening leads to the discovery of novel non-nucleotide P2Y$_1$ receptor antagonists. *Bioorg. Med. Chem. Lett.* **2012,** 20, 5254-5261.
29. Pfefferkorn, J. A.; Choi, C.; Winters, T.; Kennedy, R.; Chi, L.; Perrin, L. A.; Lu, G.; Ping, Y. W.; McClanahan, T.; Schroeder, R.; Leininger, M. T.; Geyer, A.; Schefzick, S.; Atherton, J. P2Y$_1$ receptor antagonists as novel antithrombotic agents. *Bioorg. Med. Chem. Lett.* **2008,** 18, 3338-3343.
30. Chao, H.; Turdi, H.; Herpin, T. F.; Roberge, J. Y.; Liu, Y.; Schnur, D. M.; Poss, M. A.; Rehfuss, R.; Hua, J.; Wu, Q.; Price, L. A.; Abell, L. M.; Schumacher, W. A.; Bostwick, J. S.; Steinbacher, T. E.; Stewart, A. B.; Ogletree, M. L.; Huang, C. S.; Chang, M.; Cacace, A. M.; Arcuri, M. J.; Celani, D.; Wexler, R. R.; Lawrence, R. M. Discovery of 2-(phenoxypyridine)-3-phenylureas as small molecule P2Y$_1$ antagonists. *J. Med. Chem.* **2013,** 56, 1704-1714.
31. Pi, Z.; Sutton, J.; Lloyd, J.; Hua, J.; Price, L.; Wu, Q.; Chang, M.; Zheng, J.; Rehfuss, R.; Huang, C. S.; Wexler, R. R.; Lam, P. Y. 2-Aminothiazole based P2Y$_1$ antagonists as novel antiplatelet agents. *Bioorganic & medicinal chemistry letters* **2013,** 23, 4206-4209.
32. Wang, T. C.; Qiao, J. X.; Clark, C. G.; Jua, J.; Price, L. A.; Wu, Q.; Chang, M.; Zheng, J.; Huang, C. S.; Everlof, G.; Schumacher, W. A.; Wong, P. C.; Seiffert, D. A.; Stewart, A. B.; Bostwick, J. S.; Crain, E. J.; Watson, C. A.; Rehfuss, R.; Wexler, R. R.; Lam, P. Y. Discovery of diarylurea P2Y$_1$ antagonists with improved aqueous solubility. *Bioorg. Med. Chem. Lett.* **2013,** 23, 3239-3243.
33. Ruel, R.; L'Heureux, A.; Thibeault, C.; Daris, J. P.; Martel, A.; Price, L. A.; Wu, Q.; Hua, J.; Wexler, R. R.; Rehfuss, R.; Lam, P. Y. New azole antagonists with high affinity for the P2Y$_1$ receptor. *Bioorg. Med. Chem. Lett.* **2013,** 23, 3519-3522.
34. Ruel, R.; L'Heureux, A.; Thibeault, C.; Lapointe, P.; Martel, A.; Qiao, J. X.; Hua, J.; Price, L. A.; Wu, Q.; Chang, M.; Zheng, J.; Huang, C. S.; Wexler, R. R.; Rehfuss, R.; Lam, P. Y. Potent P2Y$_1$ urea antagonists bearing various cyclic amine scaffolds. *Bioorg. Med. Chem. Lett.* **2013,** 23, 6825-6828.
35. Qiao, J. X.; Wang, T. C.; Ruel, R.; Thibeault, C.; L'Heureux, A.; Schumacher, W. A.; Spronk, S. A.; Hiebert, S.; Bouthillier, G.; Lloyd, J.; Pi, Z.; Schnur, D. M.; Abell, L. M.; Hua, J.; Price, L. A.; Liu, E.; Wu, Q.; Steinbacher, T. E.; Bostwick, J. S.; Chang, M.; Zheng, J.; Gao, Q.; Ma, B.; McDonnell, P. A.; Huang, C. S.; Rehfuss, R.; Wexler, R. R.; Lam, P. Y. Conformationally constrained ortho-anilino diaryl ureas: discovery of 1-(2-(1'-neopentylspiro[indoline-3,4'-piperidine]-1-yl)phenyl)-3-(4-(trifluoromet hoxy)phenyl)urea, a potent, selective, and bioavailable P2Y$_1$ antagonist. *J. Med. Chem.* **2013,** 56, 9275-9295.
36. Yuan, S.; Chan, H. C. S.; Vogel, H.; Filipek, S.; Stevens, R. C.; Palczewski, K. The molecular mechanism of P2Y$_1$ receptor activation. *Angew. Chem. Int. Ed.* **2016,** 55, 10331-10335.
37. Zhang, D.; Gao, Z. G.; Zhang, K.; Kiselev, E.; Crane, S.; Wang, J.; Paoletta, S.; Yi, C.; Ma, L.; Zhang, W.; Han, G. W.; Liu, H.; Cherezov, V.; Katritch, V.; Jiang, H.; Stevens, R. C.; Jacobson, K. A.; Zhao, Q.; Wu, B. Two disparate ligand-binding sites in the human P2Y$_1$ receptor. *Nature* **2015,** 520, 317-321.
38. Zhang, X.; Lu, F.; Chen, Y. K. Discovery of potential orthosteric and allosteric antagonists of P2Y$_1$R from chinese herbs by molecular simulation methods. *Evid. Based Complement. Alternat. Med.* **2016,** 2016, ID 4320201.
39. Gao, Z. G.; Jacobson, K. A. Distinct signaling patterns of allosteric antagonism at the P2Y1 receptor. *Mol. Pharmacol.* **2017**, mol.117.109660.

40. Neumann, W.; Xu, S.; Sárosi, M. B.; Scholz, M. S.; Crews, B. C.; Ghebreselasie, K.; Banerjee, S.; Marnett, L. J.; Hey-Hawkins, E. nido-Dicarbaborate induces potent and selective inhibition of cyclooxygenase-2. *ChemMedChem* **2016,** 11, 175-178.
41. Scholz, M.; Blobaum, A. L.; Marnett, L. J.; Hey-Hawkins, E. ortho-Carbaborane derivatives of indomethacin as cyclooxygenase (COX)-2 selective inhibitors. *Bioorg. Med. Chem.* **2012,** 20, 4830-4837.
42. Laube, M.; Neumann, W.; Scholz, M.; Lonnecke, P.; Crews, B.; Marnett, L. J.; Pietzsch, J.; Kniess, T.; Hey-Hawkins, E. 2-Carbaborane-3-phenyl-1*H*-indoles--synthesis *via* McMurry reaction and cyclooxygenase (COX) inhibition activity. *ChemMedChem* **2013,** 8, 329-335.
43. Miyaura, N.; Suzuki, A. Stereoselective synthesis of arylated (*E*)-alkenes by the reaction of alk-1-enylboranes with aryl halides in the presence of palladium catalyst. *J. Chem. Soc. Chem. Comm.* **1979**, 866-867.
44. Miyaura, N.; Yamada, K.; Suzuki, A. A new stereospecific cross-coupling by the palladium-catalyzed reaction of 1-alkenylboranes with 1-alkenyl or 1-alkynyl halides. *Tet. Lett.* **1979,** 20, 3437-3440.
45. Kasar, R. A.; Knudsen, G. M.; Kahl, S. B. Synthesis of 3-amino-1-carboxy-o-carborane and an improved, general method for the synthesis of all three *C*-amino-*C*-carboxycarboranes. *Inorg. Chem.* **1999,** 38, 2936-2940.
46. Lazareno, S.; Birdsall, N. J. Estimation of competitive antagonist affinity from functional inhibition curves using the Gaddum, Schild and Cheng-Prusoff equations. *Br. J. Pharmacol.* **1993,** 109, 1110-1119.
47. Guengerich, F. P. Common and uncommon cytochrome P450 reactions related to metabolism and chemical toxicity. *Chem. Res. Toxicol.* **2001,** 14, 611-650.
48. Testa, B.; Kramer, S. D. The biochemistry of drug metabolism--an introduction: Part 1. Principles and overview. *Chem. Biodivers.* **2006,** 3, 1053-1101.
49. Testa, B.; Kramer, S. D. The biochemistry of drug metabolism--an introduction: Part 2. Redox reactions and their enzymes. *Chem. Biodivers.* **2007,** 4, 257-405.
50. Testa, B.; Kramer, S. D. The biochemistry of drug metabolism--an introduction: Part 3. Reactions of hydrolysis and their enzymes. *Chem. Biodivers.* **2007,** 4, 2031-2122.
51. King, R. S. Biotransformations in Drug Metabolism. In *Drug Metabolism Handbook: Concepts and Applications*, Ala F. Nassar, P. F. H., JoAnn Scatina, Ed. John Wiley & Sons, Inc.: NJ, USA, 2008; pp 17-40.
52. Nakao, R.; Schou, M.; Halldin, C. Direct plasma metabolite analysis of positron emission tomography radioligands by micellar liquid chromatography with radiometric detection. *Anal. Chem.* **2012,** 84, 3222-3230.
53. Schroder, S.; Wenzel, B.; Deuther-Conrad, W.; Teodoro, R.; Egerland, U.; Kranz, M.; Scheunemann, M.; Hofgen, N.; Steinbach, J.; Brust, P. Synthesis, ^{18}F-radiolabelling and biological characterization of novel fluoroalkylated triazine derivatives for in vivo imaging of phosphodiesterase 2A in brain via positron emission tomography. *Molecules* **2015,** 20, 9591-9615.
54. Liu, J.; Wenzel, B.; Dukic-Stefanovic, S.; Teodoro, R.; Ludwig, F. A.; Deuther-Conrad, W.; Schroder, S.; Chezal, J. M.; Moreau, E.; Brust, P.; Maisonial-Besset, A. Development of a new radiofluorinated quinoline analog for PET imaging of phosphodiesterase 5 (PDE5) in brain. *Pharmaceuticals (Basel, Switzerland)* **2016,** 9, 22.
55. K.C. Lee, S.-Y. L., Y.S. Choe, D.I.Chi Metabolic Stability of [^{18}F]Fluoroalkylbiphenyls *Bull. Korean. Chem. Soc* **2004,** 25, 1225-1230.
56. Ferguson, C. S.; Tyndale, R. F. Cytochrome P450 enzymes in the brain: emerging evidence of biological significance. *Trends Pharmacol. Sci.* **2011,** 32, 708-714.
57. Coenen, H. H.; Laufer, P.; Stöcklin, G.; Wienhard, K.; Pawlik, G.; Böcher-Schwarz, H. G.; Heiss, W. D. 3-*N*-(2-[^{18}F]-fluoroethyl)-spiperone: A novel ligand for cerebral dopamine receptor studies with pet. *Life Sci.* **1987,** 40, 81-88.
58. Welch, M. J.; Katzenellenbogen, J. A.; Mathias, C. J.; Brodack, J. W.; Carlson, K. E.; Chi, D. Y.; Dence, C. S.; Kilbourn, M. R.; Perlmutter, J. S.; Raichle, M. E.; et al. *N*-(3-[^{18}F]fluoropropyl)-spiperone:

the preferred ^{18}F labeled spiperone analog for positron emission tomographic studies of the dopamine receptor. *Int. J. Rad. Appl. Instrum. B* **1988,** 15, 83-97.
59. Wenzel, B.; Mollitor, J.; Deuther-Conrad, W.; Dukic-Stefanovic, S.; Kranz, M.; Vraka, C.; Teodoro, R.; Günther, R.; Donat, C. K.; Ludwig, F.-A.; Fischer, S.; Smits, R.; Wadsak, W.; Mitterhauser, M.; Steinbach, J.; Hoepping, A.; Brust, P. Development of a novel nonpeptidic ^{18}F-labeled radiotracer for in vivo imaging of oxytocin receptors with positron emission tomography. *J. Med. Chem.* **2016,** 59, 1800-1817.
60. Kirchmair, J.; Goller, A. H.; Lang, D.; Kunze, J.; Testa, B.; Wilson, I. D.; Glen, R. C.; Schneider, G. Predicting drug metabolism: experiment and/or computation? *Nat. Rev. Drug Discov.* **2015,** 14, 387-404.